

Development of the Solar Array Deployment and Drive System for the XTE Spacecraft

Rodger Farley* and Son Ngo*

Abstract

The X-ray Timing Explorer (XTE) spacecraft is a NASA science low-earth orbit explorer-class satellite to be launched in 1995, and is an in-house Goddard Space Flight Center (GSFC) project. It has two deployable aluminum honeycomb solar array wings with each wing being articulated by a single axis solar array drive assembly. This paper will address the design, the qualification testing, and the development problems as they surfaced of the Solar Array Deployment and Drive System.

Introduction

The XTE spacecraft will be carried into orbit on a Delta II expendable rocket, and the solar arrays will remain folded until the spacecraft is off the Delta second stage. The two silicon-celled wings are comprised of three panels each, with a total array area of 17.88 m² (192.5 ft²). Figure 1 shows the panels stowed and deployed. By a timer sequence on the spacecraft, the two wings are deployed by initiating the pyrotechnic pin pullers in the release mechanisms. Kick-off springs initiate the first motion to break the stiction and spring driven hinges with rotary viscous dampers carry the panels to their deployed positions minimizing the kinetic energy. Limited travel of ± 90 deg was required to articulate the arrays, and this was accomplished with a solar array drive composed of a main hinge, a stepper motor based rotary actuator, and a rotary cable wrap to transfer power and sensor signals from the array.

Some of these mechanisms were an outgrowth of the devices designed for the COBE spacecraft. What was attempted early on in the preliminary design of the solar array and antenna deployment systems was to use the same or similar components not only between the two subsystems, but also between two spacecraft, namely XTE and the Tropical Rainfall Measurement Mission.

The qualification program progressed to a very late date before problems became evident, most notably unusual wear in the harmonic drive of the rotary actuator, G-negation imbalance during deployment tests, and honeycomb panel face sheet delamination of the flight solar array panels.

* NASA Goddard Space Flight Center, Greenbelt, MD

Component Descriptions

Solar Array Drive Assembly

The Solar Array Drive Assembly, or SADA, consisted the three main subassemblies: the Rotary Actuator, the Cable Wrap, and the Main Deployment Hinge. Figure 2 shows a cross section of this device.

The Rotary Actuator is a Schaeffer Magnetic's modified type 5 actuator with an output bearing from a type 6 drive, thus it was called a type 5 and 1/2. It is a three-phase, six-state stepper motor with a 200:1 reduction gear harmonic drive. The harmonic drive was a "silk hat" type with a pitch diameter of 6.35 cm (2.5 in). Materials for the harmonic drive are as follows: the flexspline is 304L stainless steel, the circular spline is 17-4 PH stainless steel, and the wave generator bearing is 440C stainless steel. The gear teeth and bearings were lubricated with Penzane 2000 synthetic hydrocarbon oil, with a 5% lead naphthanate additive as well as an antioxidant. An internal rotary incremental encoder with three absolute positions provided position, velocity, direction of travel, and could be used in a closed or open loop mode. The encoder used pairs of light emitting diodes and photo transistors on several tracks. A circular disk with a punch-out pattern placed between the diodes and transistors provided the logic signals.

The Cable Wrap is a device in which individual hook-up wires have been sewn together to form two belts that spiral around a central reel. This two arm spiral wrap communicates 76 wires (mostly 20 gage) across the rotary joint, and in addition (in their own separate chambers) two twisted shielded pair wires for the coarse sun sensors on the arrays. The spiraling parts of the two belts are each 0.914 m (36 in) long and 6.35 cm (2.5 in) wide, with the inner diameter of the reel being 4.19 cm (1.65 in), and the outer diameter of the reel being 13 cm (5.12 in). The two main belts are separated by a sheet of 127 μm (0.005 in) thick Kapton, which greatly smooths the sliding friction between the two belts and their Dacron stitches. A "twill weave lock stitch" was used to sew the wires together. The reel and housing were aluminum with an anodized/Teflon coating. The cable wrap has a maximum travel of ± 300 deg (where it either winds completely on the inner diameter or out on the outer diameter), but the designed use is between ± 175 deg where it can operate in the "sweet spot" region of low friction. Maximum design travel is estimated by relationships written in Figure 2.

The Main Deployment Hinge bolts onto the output face of the rotary actuator, and rotates the wing 90 deg from the spacecraft body. It does this with constant torque spring laminates and a rotary viscous damper, kept warm with strip heaters and thermostats. A delay latch connected to the extension of the locking latch prevents the three panels from their final deployment until the main hinge has rotated the wing at least 85 deg. This hinge also carries the thrust launch loads of the outer solar array panel.

Panel to Panel Hinges

These hinges have spherical bearings to accommodate misalignments and distortions, and act as a redundant rotary path. These hinges are installed in pairs with one fixed, the other free to float along the hinge line. One hinge of the pair has a rotary viscous damper (same as the main hinge) and the other hinge has a rotary potentiometer for position telemetry.

Honeycomb Panels

The panels are made from 7075 T73 aluminum face sheets, 180 μm (0.007 in) thick. The overall panel thickness is 2 cm (0.787 in) and outside dimensions are 1.067 m x 2.79 m (42 x 110 in). The aluminum core density is 32 kg/m^3 (2.0 lb/ft^3) with a cell size of 4.8 mm ($3/16$ in). The FM123-2LVC adhesive was selected for its low outgassing qualities and history of use at the GSFC. The lowest density film was used. The panels have internal doublers and machined blocks. One side of each panel was insulated with 152 μm (0.006 in) of ED-3, a type of E-glass fiberglass.

Release Mechanisms

The retention/release mechanisms have at their heart pyrotechnic HiShear pin pullers with 6.35 mm (0.25 in) diameter pins that could retract with a 4003 N (900 lb) single shear side force. Three jaws hold a tension/release rod with a conical end, and two of the three jaws were restrained with pin pullers. Release can occur with the retraction of one out of the three jaws. The tension/release rods would compress a series of cones and vee guides, with preloads selected to allow expansion and sliding of the panels (Figure 3). The degrees of constraint were selected in order to isolate it from spacecraft generated loads which could damage the arrays. The cones and vees were made from titanium with a titanium oxide / Teflon coating, although upon reflection a better choice perhaps would have been aluminum with an aluminum oxide / Teflon coating to lessen the chance of galling and increase workability for shear pin installation. Braycote 602 grease was used liberally on the interfaces.

Qualification Program Overview

The qualification of the system consisted of components that had undergone testing, building up to a full assembly qualification test program. This included vibration, acoustic, ambient deployment, cold deployment, hot deployment, and torque margin deployment tests. In parallel to these efforts, life tests of the cable wrap, the actuator, and the SADA were performed to address the wear issues.

System Test Methods

The most interesting part of the test program was the full up deployments of the solar array wing. With G-negation consisting of a combination of airpads and counter weights, a full, uninterrupted, end to end deployment of all the hinge axes could be accomplished in one test in the same manner as the anticipated flight deployment.

Early in the program it was recognized that the air pad system would have to compensate for a hinge axis that was close but not perfectly parallel to gravity. If the solar array wing wanted to climb up hill during a deployment test due to an imperfectly

aligned hinge, the required change in potential energy would have to be supplied by the hinge springs. That of course was unacceptable because the springs did not have that much stored energy to spare, resulting in a loss of torque available to swing the wing out. Instead, the energy should be supplied by the airpad suspension system. The airpad assembly would have, in addition to the airpads, a cylinder/piston arrangement. Air pressure controlled by a regulator would float the piston and anything it had to support (such as a solar array) with a constant force. The rise or fall of the piston during the deployment could compensate for a misaligned hinge. What is necessary and easy to control is that the airpad table be very level. Figure 4 shows this arrangement. The constant force desired could be achieved by either multiplying the piston area with the air regulator pressure, or by monitoring the set of strain gages that was applied to the support tube between the piston and the load. This tube was made thin enough in order to make the strain a measurable amount. Swales and Associates, Inc., a local support contractor designed this air pad system.

Producing full deployments under thermal conditions posed a great challenge, and a compromise allowed a practical solution. The compromise was to simulate flight temperatures and gradients while in the stowed configuration, and to release thermal control just before and during deployment. This was accomplished with a thermal insulating box encapsulating the array, and was controlled by liquid nitrogen and heaters. Two thermal circuits helped to produce the desired gradients, although the magnitude of the panel to panel gradients were not achieved. When the bulk temperatures and gradients were sustained for some minutes, the thermal box lid was quickly removed and the pyro pin pullers were subsequently fired.

Torque margin verification was simply demonstrated by removing 50% of all hinge springs and timing the deployment. Each hinge line had two springs, and so removing one spring per hinge line produced the desired deficiency. The result was that the deployment took about twice as long, indicating that the Coulomb friction in the system was a small fraction of the spring force available. This demonstrated a torque margin greater than 2, and by implication of the deployment speed and a known damping rate, a much higher calculated margin can be said to exist.

Torque margin verification of the rotary actuator was done by a combination of test data and modeling. Since the device uses a 200:1 reduction gear, the margin to be concerned with in our case was the internal torque margin at the motor rotor. Since applying an internal brake force to "dial up the load" to measure torque margin was impossible, test data of the input friction vs temperature had to be measured and modeled instead. This was done on the qualification unit motor rotor and harmonic drive, lubricated with Penzane 2000 on a test stand. The temperature was varied from 50 deg C to -20 deg C. Schaeffer Magnetics provided this crucial data, which was incorporated into a GSFC-generated computer program called Mosim. The program could "dial up" this friction map to see the resulting effect of the dynamics of the rotor over different temperatures. With the solar array inertia tuned at 1 Hz, the program predicts a margin of 3 while at -5 deg C (Figure 5). What was interesting to note, since the harmonic drive error was also modeled, was that the 2 per revolution harmonic drive error produced a 1 Hz sinusoidal output at 120 pulses per second (PPS) superimposed onto the steady motion. This predicted result was clearly demonstrated

during testing with a tuned simulator bolted to the output flange. A very strong coupled response between 105 and 135 PPS resulted. The speed had to be within 10 PPS of the center frequency for the response to grow. Of course we needed additional confidence of Mosim's power to predict, and this was done by comparing the running torque vs speed test results, as well as matching the motor rotor ringing motion at temperature. This was accomplished in an indirect fashion by measuring the back EMF of the redundant motor windings while running at low speeds such as 10 PPS. Mosim would predict the voltage trace between two phases and a comparison made to test voltage data. Also the predicted current trace in one active phase could be compared to test data at low and high speeds such as 10 and 200 PPS. The characteristics to compare were the wave form shapes, frequency, amplitudes, and decay rate (low speed only). Additional tests to compare would be predictions of the threshold voltages at 28 and 200 PPS. Figures 6, 7, and 8 show some typical simulation results. It is of paramount importance that the effects of the drive electronics be incorporated into any simulation model of a stepper motor actuator, as the shape of the current pulses can have a drastic effect on the high speed torque capability.

Problems Encountered and Solutions

Harmonic Drive

Upon the completion of the rotary actuator qualification unit partial life test, no outwardly signs of deterioration could be detected by any of the tests designed to monitor health (threshold voltage, output torque). But when the unit was dismantled for inspection, it was discovered that a significant amount of wear had occurred in the harmonic drive, especially in the bearing to flexspline interface, which was unprecedented. The gear teeth were partially worn as well. The 304L flexspline inner diameter had galled with the 440C bearing outer race, the inner race had slipped down the wave generator plug, and the surfaces seemed to be dry of the original film of Penzane 2000 oil. Surely a number of things had gone wrong here. A number of theories were put forth, but of course nothing could be proven to satisfaction due to the constraints of time and money. But a few general intuitions could be stated; the 304L flexspline was too soft a material to be put directly into service under a minimal lubrication environment (as in typical spaceflight applications). Some form of breaking-in procedure to first work harden the surfaces would have helped. The 440C bearing was not of the vacuum melt material variety, and the outer race surface was rough looking and probably had inclusions and carbide particles on the surface. The inner race should have been locked into position with a shoulder machined into the wave generator plug to prevent the bearing from being swallowed further down the flexspline throat. The factory preload produced an unusually high torsional stiffness (between 28250 and 33900 $\text{N}\cdot\text{m}/\text{rad}$ (250,000 and 300,000 $\text{in}\cdot\text{lb}/\text{rad}$)) which would indicate that the bearing stresses were higher than normally seen in service. Also, the oil did not seem very inclined to wet the surface of the 304L flexspline, and would have benefited from a grease dam to keep what little was there on the contact surface. A combination of all these effects and probably others not imagined contributed to the failure.

The tested solution, given the time constraints, was to use the commercial grade AISI 4340 steel flexspline and 52100 steel wave generator bearing. Gold plating was

seriously considered to prevent possible corrosion of the 4340 steel, but was later rejected due to the concerns of the ability to properly gold plate, and the realization that if any corrosion occurred, it would be more cosmetic than damaging. The 52100 material was selected as a superior bearing, and under magnification had a much smoother appearance on the outer race/flexspline interface. The corrosion concern was considered minimal due to the high chrome content and the oil's antioxidant. A great effort was made to lower the preload such that the torsional stiffness would fall around $13560 \text{ N}\cdot\text{m}/\text{rad}$ ($120000 \text{ in}\cdot\text{lb}/\text{rad}$), instead of the high values of the previous set. This meant careful grinding of the wave generator plug major axis. The plug was further modified by machining a shoulder to register the inner race, thereby giving a hard load path for the reaction to the walking forces which tend to draw in the wave generator when acting as a speed reducer. Also, the oil was mixed with the grease variation of Penzane 2000 (known as Rheolub 2000) to form a slurry. This was done as it was noticed that the grease alone did not seem to release oil to keep a surface wet after it was pumped out of the contact zone. The peanut-butter like consistency was just to thick for the application, and the oil alone was just too thin. Figure 9 shows the application of the different forms of Penzane on the harmonic drive. Initial testing was done in ambient conditions in order to quickly weed out the nonsolutions. Testing in ambient conditions was seen with some doubt, since the presence of oxygen could alter the results either way. The metals would benefit from oxygen in that any wear would expose fresh metal that could quickly gall if surface oxidation did not occur first, creating a ceramic layer separating the metals. The oil, on the other hand, would be stressed in the presence of oxygen, and in fact the oil turned darker and chemical analysis indicated some oxidation had occurred. Further testing in vacuum vindicated both the oil/grease slurry and the material combination.

G-negation

As stated earlier, a combination of airpads and counter weights were used to deploy a wing assembly. The more complicated components were by far the airpads, but the greatest problems occurred with the counter weights. This in part was due to deflections of the counter weight brackets, but was mostly due to panel deflections which varied with the deployment angle. With the springs disabled, measured values of counter weight unbalance exceeded $5.6 \text{ N}\cdot\text{m}$ ($50 \text{ in}\cdot\text{lb}$). This unbalance could shift from positive to negative maximums in as little as a 30 deg motion. Since this was over 150% of the spring force available, it presented quite a problem. The solution was to control the deflections of the panel by using an auxiliary hinge, which kept panel tip deflections to a minimum by constraining the vertical motion of the deploying panel to the stationary middle panel. The constraint loads would react in an in-plane direction of the middle panel, which is the stiffest load path, and therefore produce the least deflection. Balance error was reduced to 10% of the original error.

Release Mechanism Galling

The vee guide interface to the spacecraft (qualification unit) was knowingly installed with a slight misalignment in order to see if any galling of the two surfaces would occur during vibration, and if any such galling would hang up the deployment. The vee guides were titanium with an anodic / Teflon coating, and had Braycote 602 grease applied at the interface. Even though one of the spacecraft interfaces was a cone, there was much relative motion in the vee guide, with some displacements being on

the order of ± 2.5 mm (0.1 in) during the in-plane sine vibration test. After the vibration test, an ambient deployment test was performed. The deployment first begins with the pyro shock followed by the four kick-off springs, each 22.2 N (5 lbf). Another source of potential energy was the panels themselves, as they were slightly bowed due to the preload of the snubbers. This preload would produce a reaction load of 311 N (70 lbf) at each release mechanism, bringing the total force to break contact after the pin pullers fired to 355 N (80 lbf). After the test, the vee guide contact surface was examined and the result was that a small area of the surface coating had been worn off on both mating surfaces, exposing bare titanium. A very small area inside that area (perhaps 1 x 1 mm) had a peculiar, porous surface texture, as if some micro welding and tearing had occurred. Whether the galling had resulted in a firm weld or a broken weld at the end of the vibration test, that could not be determined. However, with 355 N (80 lbf) and a pyro shock right at the vee guide, the resultant initial motion was quite aggressive, galled or not. The saving grace is that the flight units are shimmed to perfection to avoid any high contact stresses which are required for galling.

Honeycomb Panels

The qualification solar array wing had been exposed to the full engineering test qualification program without any structural problems. But the flight units, during their bake out at temperatures slightly above 100 deg C, delaminated over large areas where there were internal doubler sheets. The delaminations seemed to develop thru a low adhesion to the doubler and combined with a gas generated from the adhesive itself. The delaminated face sheet was blistered up in a permanently yielded condition, as if internally pressurized. The possibilities for the source of the problem seemed endless, such as contamination, tooling, handling, humidity, tolerance buildup, primer, and so on. The truly frightening aspect was that tap testing did not detect the problem of "light bonding." Sophisticated techniques such as pulse echo and air scanning failed to detect lightly bonded areas adjacent to the obviously failed spots which later were determined to be lightly bonded as well. There were too many layers in the solar array panel to image separately. The best interrogative method was to grind a small hole in the external face sheet, exposing the doubler underneath, and to push a dental pick into the adhesive between the two aluminum sheets. If the parts were lightly bonded, the metal skins would separate. If the dental pick could not be shoved into the adhesive layer without tearing the face sheet or bending the pick, then the adhesive was considered acceptable.

Since the failure occurred in three out of the six panels in virtually the exact same areas implicating tooling, tolerance, and process, the speculation on the cause narrows to the following argument. The process of handling this adhesive film included numerous thawing and refreezing cycles between use and storage. Together with high environmental humidity, the adhesive could have absorbed water from these types of exposure. In parallel, the mechanical tolerances had to be kept tight in order to prevent a low cure pressure situation, where the outer face sheet would have to arch down to make contact with the already assembled and cured internal doubler panel. If a thick caul plate (top tooling plate) was used, the autoclave pressure would have to deform it also as it bridged across the doubler panel. These conditions lead to low cure pressure locally over the internal doubler panel. Unfortunately the adhesive film is sensitive to this condition as it has a very low-flow

nature, a definite disadvantage of the adhesive. So, if the adhesive was poisoned by moisture and aggravated by low curing pressures, and trapped in a sheet to sheet bond where products of curing or outgassing water vapor had to travel sideways thru the adhesive layer, and not simply straight out into the vented honeycomb core, then "light bonding" should not be an unexpected result. Over the core away from the doubler panels, products of curing easily escaped into the vented core, and there were no bridging problems here, and so these areas did not suffer from the sensitive nature of the adhesive or moisture absorption.

The fix was to grind and strip all the lightly bonded areas and with a hand layup, apply custom cut face sheet material with EA9395 epoxy. To have prevented the problem all together would entail a close examination on the requirements to use of FM123-2LVC, the vendor's capability and successful history of using that product, and a high appreciation of the delicate and unforgiving nature of that film adhesive which requires expert handling.

Conclusions

Nothing should be taken for granted! Most of the areas we anticipated to be problems were not, and many unexpected areas became major problems. An entire subsystem such as a solar array deployment and drive entail hundreds of details, many of which take care of themselves. Lubrication and process controls of even typical everyday applications should never be taken as givens. Cheaper, faster will usually result in many details falling thru the cracks, and then it is a gamble whether these details take care of themselves, or not.

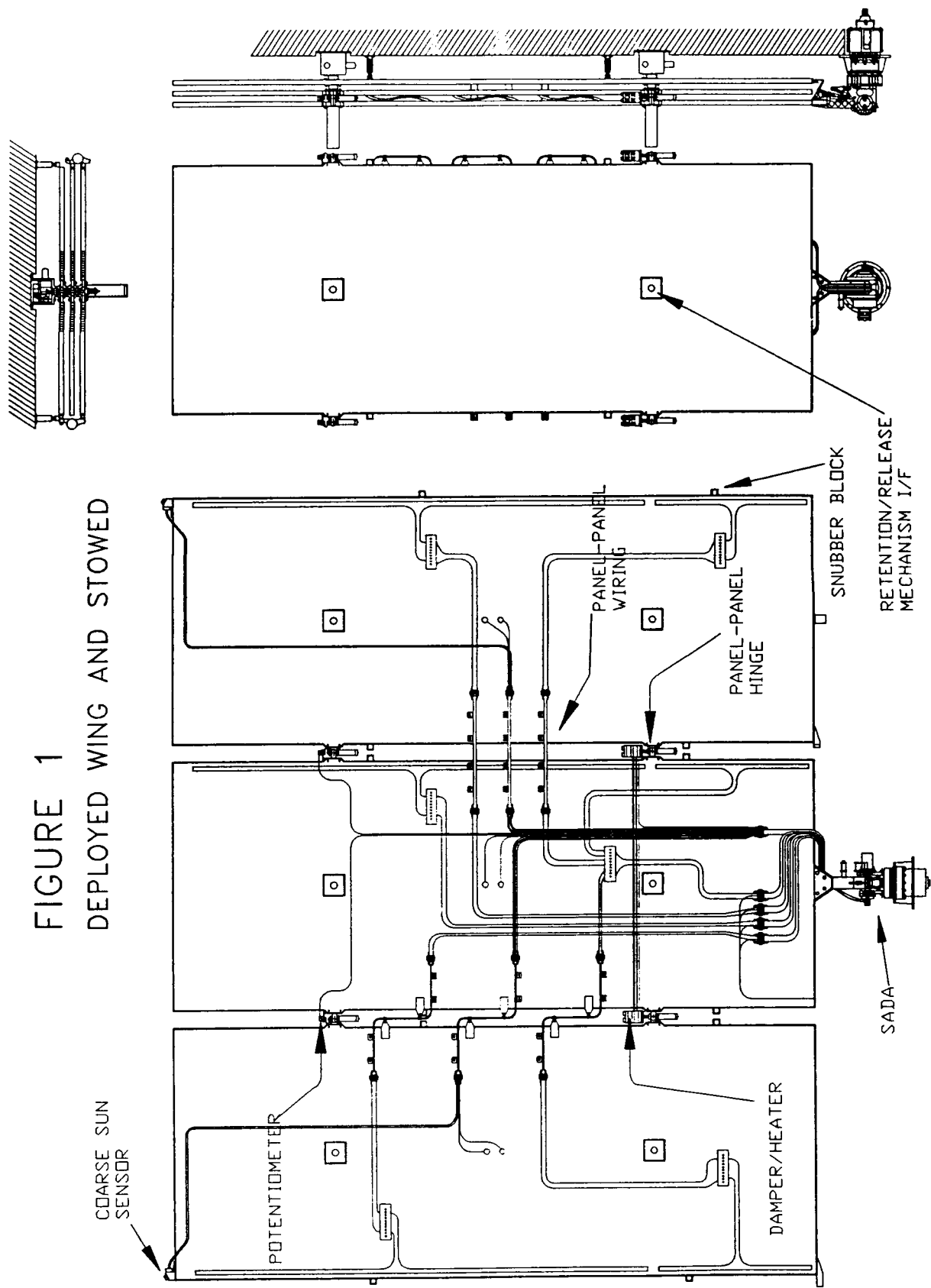


FIGURE 1
DEPLOYED WING AND STOWED

FIGURE 2 XTE SADA

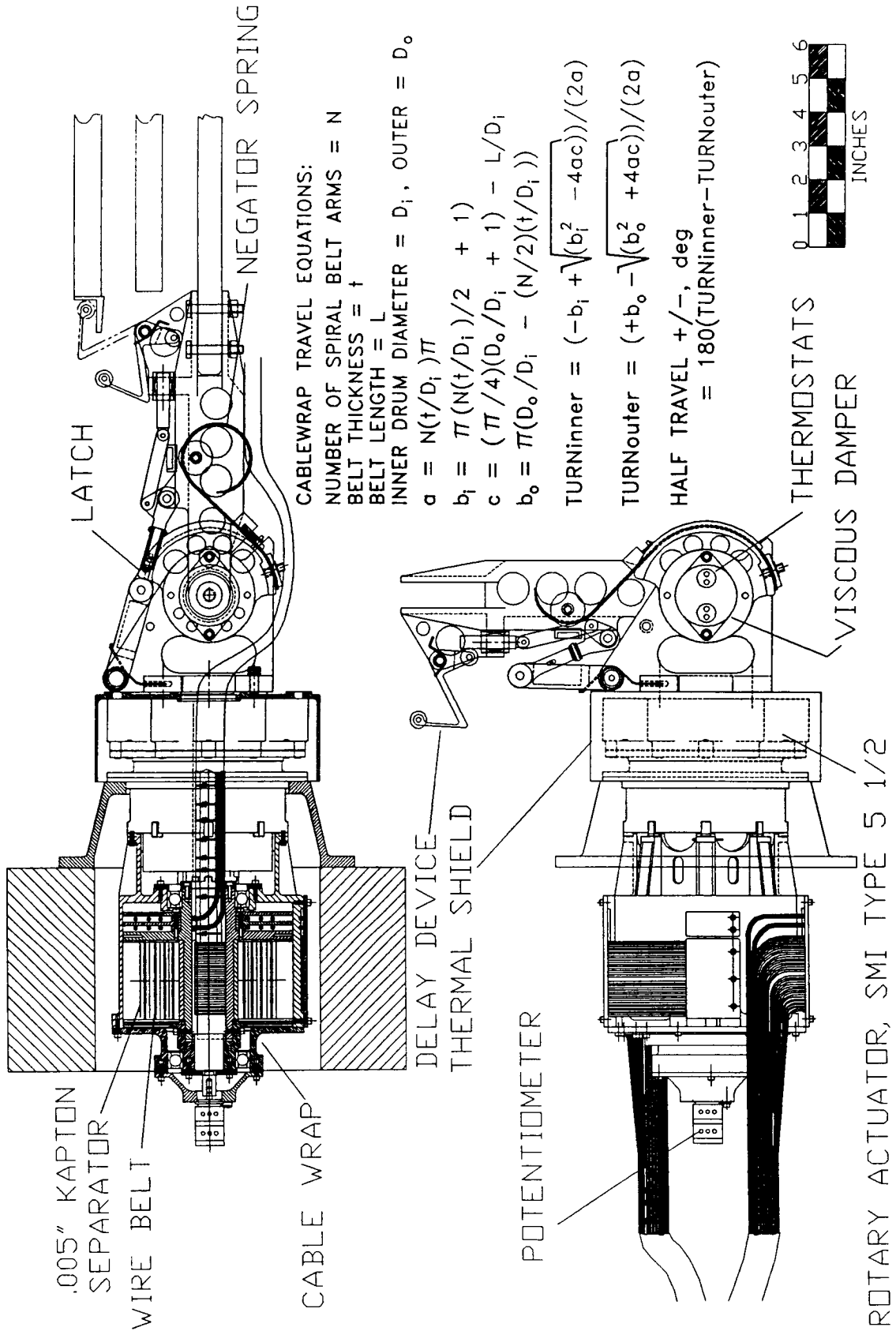


FIGURE 3 XTE S/A RETENTION/RELEASE MECHANISM

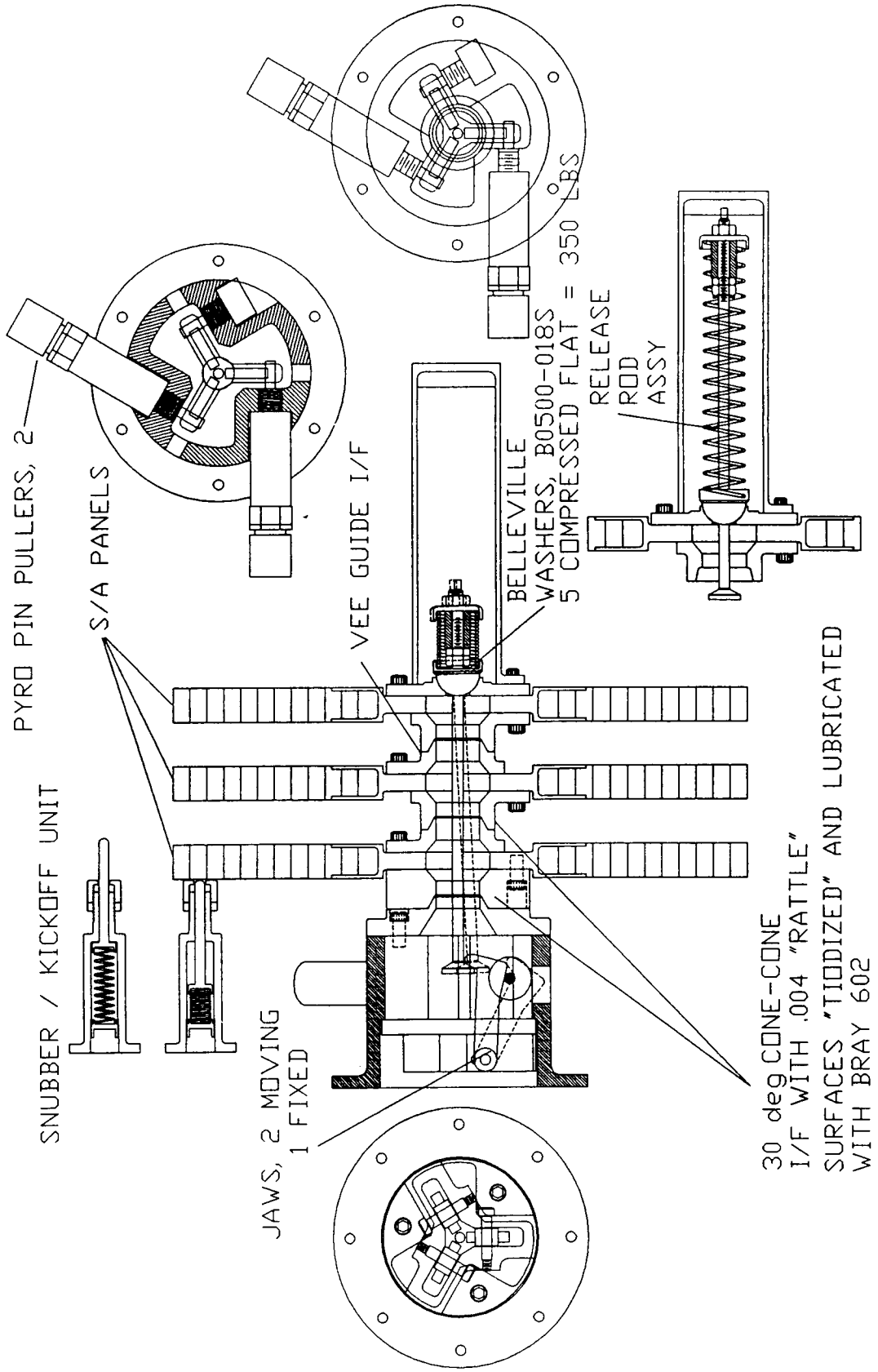
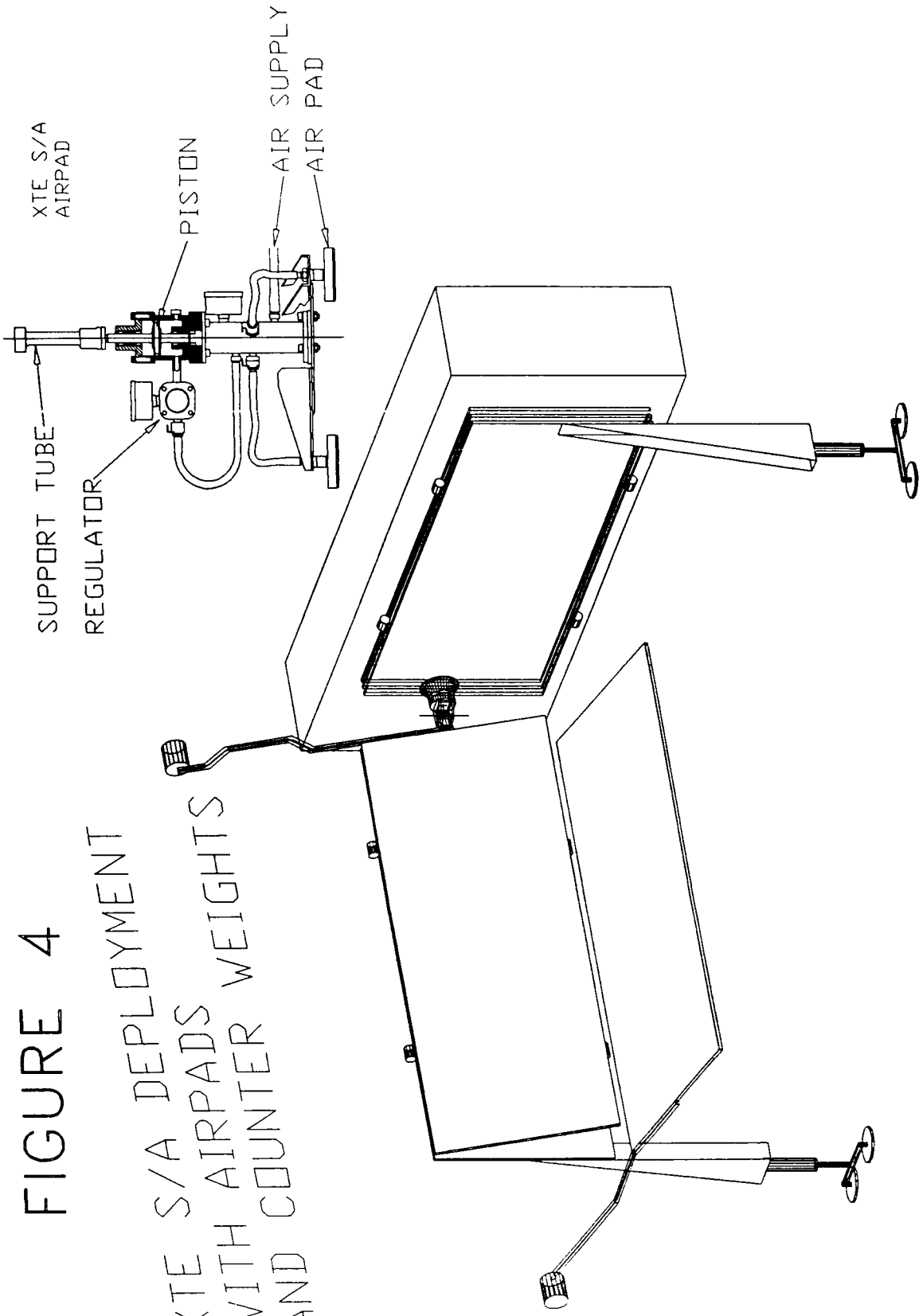
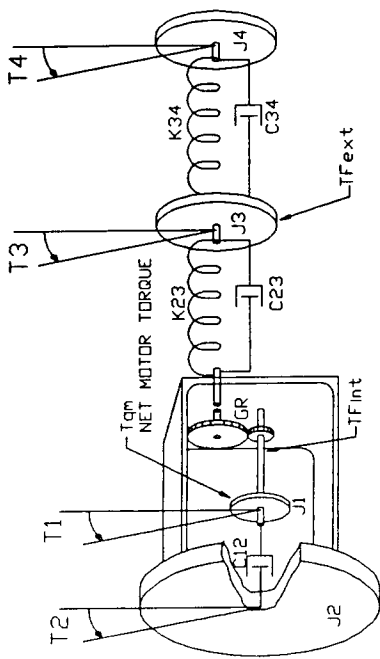


FIGURE 4
XTE S/A DEPLOYMENT
WITH AIRPADS
AND COUNTER WEIGHTS



ROTARY ACTUATOR MODEL
DEFINITION OF VARIABLES



ROTARY ACTUATOR MODEL
DEFINITION OF COMPONENTS

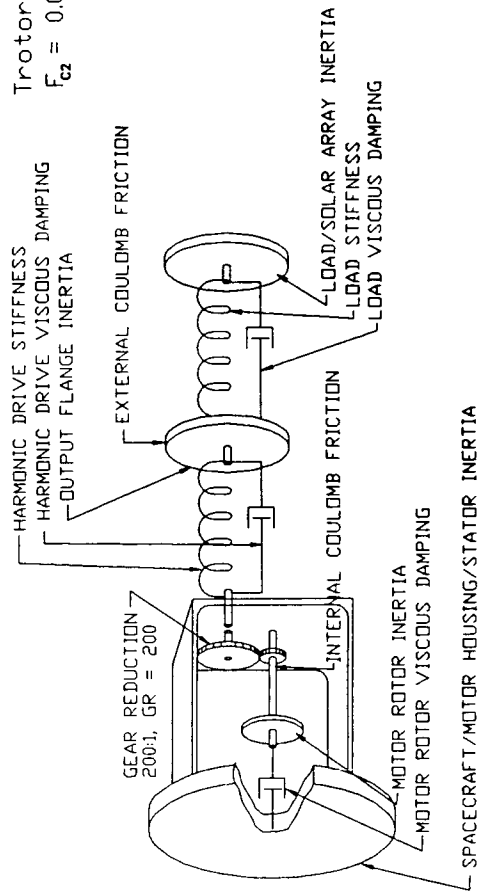


FIGURE 5

DIFFERENTIAL EQUATIONS

$$\ddot{T}_1 = \{-K23*(T3-T2*(1+1/GR))+T1/GR - GearError\}/GR - C12*(\dot{T}_1-\dot{T}_2) - C23*(\dot{T}_3+\dot{T}_2*(1+1/GR) - \dot{T}_1/GR)/GR + Tqm - TFint\} / J1$$

$$\ddot{T}_2 = \{K23*(T3-T2*(1+1/GR))+T1/GR - GearError\}/(1+1/GR) + C12*(\dot{T}_1-\dot{T}_2) + C23*(\dot{T}_3+\dot{T}_2*(1+1/GR) - \dot{T}_1/GR)*(1+1/GR) - Tqm + TFint + TFext\} / J2$$

$$\ddot{T}_3 = \{-K23*(T3-T2*(1+1/GR))+T1/GR - GearError\} + K34*(T4-T3) + C34*(\dot{T}_4-\dot{T}_3) - C23*(\dot{T}_3+\dot{T}_2*(1+1/GR) - \dot{T}_1/GR) - TFext\} / J3$$

$$\ddot{T}_4 = \{-K34*(T4-T3) - C34*(\dot{T}_4-\dot{T}_3)\} / J4$$

$$GearError = F_{c2} \sin(2Trotor) + F_{c4} \sin(4Trotor) + F_{c9} \sin(9Trotor)$$

$$Trotor = T1 - T2$$

$$F_{c2} = 0.00025 \text{ radians} \quad F_{c4} = 1/2 F_{c2} \quad F_{c9} = 1/5 F_{c2}$$

INTERNAL FRICTION MODEL
AS FUNCTIONS OF SPEED, TEMPERATURE

$$TFint = A1*(PPS^A2)*10^{(-A3*(TEMP + A4))} + TFint @ AMBIENT, BREAKAWAY \quad in-oz$$

$$A1 = 0.55$$

$$A2 = 0.6$$

$$A3 = 0.021$$

$$A4 = 8.0$$

$$TFint @ AMBIENT, BREAKAWAY = 4 \text{ in-oz}$$

PPS = PULSES PER SECOND, AT 1.5 DEG PER PULSE
TEMP = TEMPERATURE @ DEG CENTIGRADE

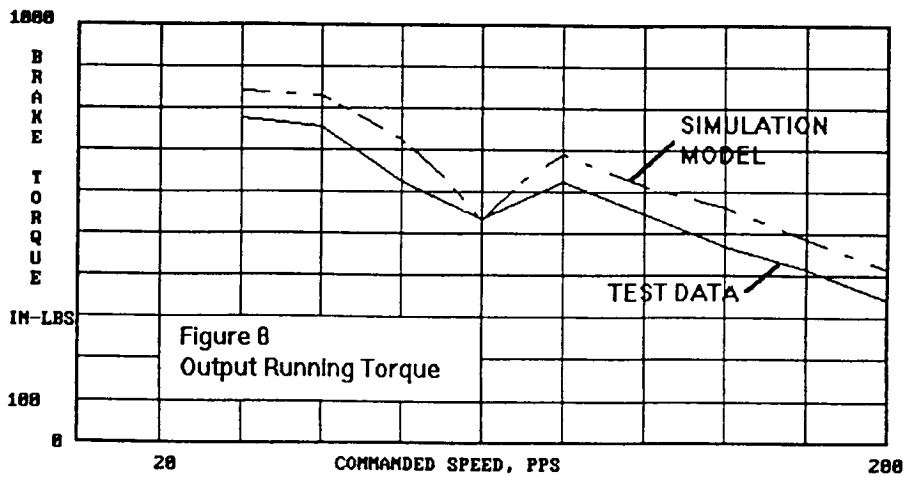
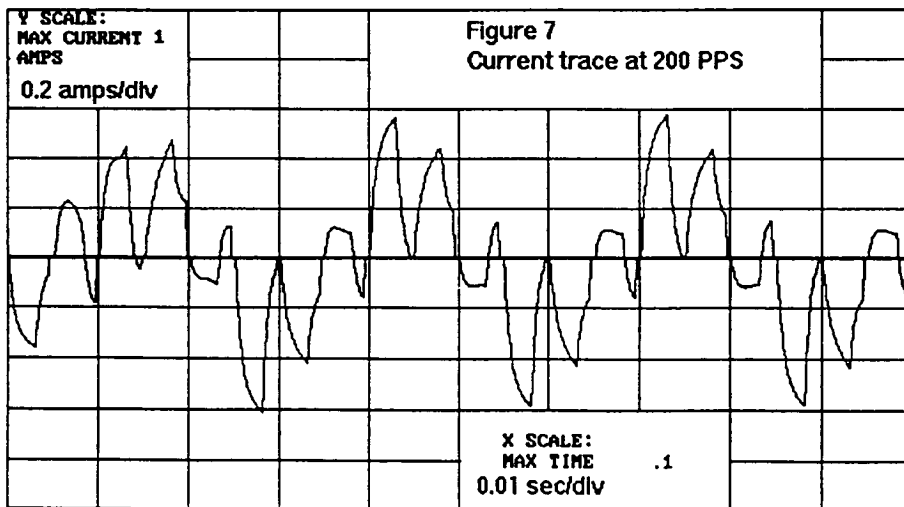
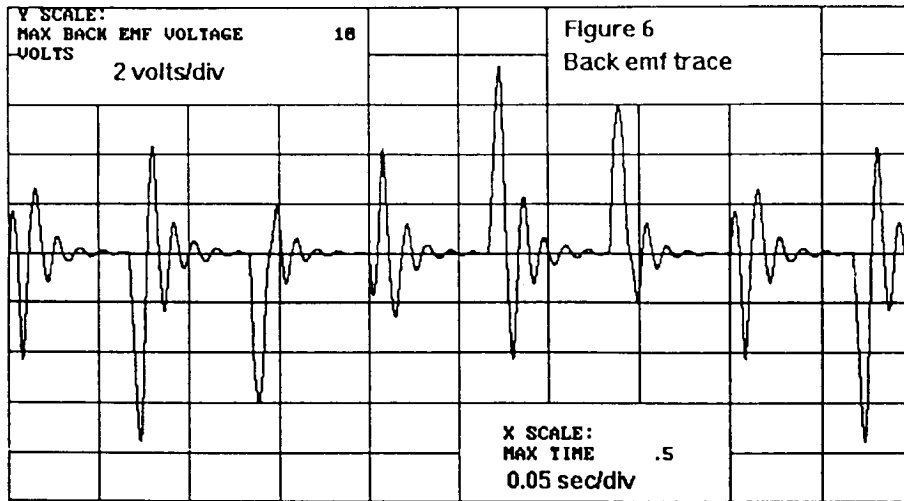


FIGURE 9
HARMONIC DRIVE FIX

